

# Thermal and Electrical Characterizations of Ultra-Thin Flexible 3YSZ Ceramic for Electronic Packaging Applications

Xin Zhao<sup>1</sup>, K. Jagannadham<sup>1</sup>, Wuttichai Reainthippayasakul<sup>2</sup>, Michael. T. Lanagan<sup>2</sup>, Douglas C. Hopkins<sup>1</sup>

<sup>1</sup>North Carolina State University

1791 Varsity Dr.

Raleigh, NC 27606

Ph: 919-513-5929; Fax: 919-513-0405

<sup>2</sup> Pennsylvania State University

N329 Millenium Science Complex

University Park, PA 16802

Email: [xzhao20@ncsu.edu](mailto:xzhao20@ncsu.edu), [kasichai@ncsu.edu](mailto:kasichai@ncsu.edu), [wyr5024@psu.edu](mailto:wyr5024@psu.edu), [mxl46@psu.edu](mailto:mxl46@psu.edu), [dchopkins@ncsu.edu](mailto:dchopkins@ncsu.edu)

---

## Abstract

This paper presents thermal and electrical characterizations of an ultra-thin flexible 3YSZ (3 mol% Yttria Stabilized Zirconia) ceramic substrate to explore its potential for electronic packaging applications. The thicknesses of the ultra-thin 3YSZ substrates were 20  $\mu\text{m}$  and 40  $\mu\text{m}$ . The flexible thin ceramic substrate can provide not only better modulus for higher robustness in manufacturing, especially in Z-axis direction of modules, but also low thermal resistance for high density 2D (two dimensional) / 3D (three dimensional) power module packaging applications. To better understand the thermal and electrical properties of the ultra-thin flexible ceramic, different measurements were employed. Thermal conductivity was measured at different temperatures by 3-omega method, the results were verified by thermo-reflectance measurement at room temperature. Relative permittivity was measured from 100 Hz to 10 MHz, with dielectric losses determined by dielectric spectroscopy. The dielectric breakdown of the ultra-thin flexible 3YSZ was measured, from room temperature to 150  $^{\circ}\text{C}$ . Weibull analysis was performed on 20 measurements for each temperature. The test results showed that the thermal conductivity of 3YSZ decreased from 3.3 W/mK at 235 K to 2.2 W/Mk at 600 K. The relative permittivity decreased from 30.9 to 27.3 for higher frequencies for both substrates with different thickness. The temperature-dependence of relative permittivity and dielectric loss was studied. The results showed that these two parameters increased slowly from -65  $^{\circ}\text{C}$  to 150  $^{\circ}\text{C}$ , but more rapidly from 175  $^{\circ}\text{C}$  to 250  $^{\circ}\text{C}$ . The dielectric breakdown decreased at higher temperature, from 5.76 kV to 2.64 kV for thickness of 20  $\mu\text{m}$ , 7.84 kV to 3.36 kV for thickness of 40  $\mu\text{m}$ . SEM (Scanning Electron Microscopy), EDS (Energy-dispersive X-ray Spectroscopy) and XRD (X-ray Powder Diffraction) analysis was performed to compare the microstructure of 3YSZ ultra-thin substrate and that of AlN (Aluminum Nitride) substrate. The microstructure of 3YSZ consisted of smaller round particles and that of AlN contained larger columnar particles. FEA (Finite Element Analysis) simulations were also applied to demonstrate the thermal properties of 3YSZ in simplified model of power modules. Though the measurement results showed that it did not meet expectations for high temperature power modules, the present work showed potential applications of the ultra-thin 3YSZ substrates in low voltage power modules, LED modules.

## Key words

ultra-thin 3YSZ, flexible substrate, electronic packaging, thermal conductivity, dielectric breakdown, relative permittivity

---

## I. Introduction

The dielectric substrate and interposer are important components in electronic packaging for different applications, such as power modules, LED modules or 3D Integrated Circuits packaging. The substrate and interposer

provide not only an assembly and interconnections platform for heterogeneous integration of electrical components, circuits and structures, but also mechanical, thermal and electrical interfaces between different parts of the systems [1] - [3]. Though the state of art packaging on rigid

substrates is favored for various applications, the demand for packaging with ultra-thin flexible substrates is growing for better mechanical and thermal management in engineering areas such as optoelectronics [4] – [5]. A thin flexible substrate offers an additional advantage to improve power density in power modules by smaller size. Hence, the potential application of thin flexible substrates to power electronics are being explored [6] – [8].

With good chemical and structural stability, high mechanical strength and compatibility with other materials, YSZ has also been studied, and applied for micro-tubular solid oxide fuel cells (MT-SOFCs) [9] – [10]. Studies also indicated that 8YSZ has with higher electrical conductivity at intermediate temperature, while 3YSZ offers superior mechanical properties with ~ 1200 MPa bending strength (~ 230 MPa for 8YSZ) [11]. Though the thermal conductivity of 3YSZ is low compared with that of aluminum nitride (AlN) or aluminum oxide [12], the recent commercialized ultra-thin (20  $\mu\text{m}$ , 40  $\mu\text{m}$ ) flexible 3YSZ substrates, provided by ENrG Inc., showed its comparable low thermal mass for electronic packaging applications.

In this paper, SEM and EDS analysis was applied to compare the microstructure of the ultra-thin flexible 3YSZ substrate and that of conventional AlN substrate. The relevant properties of the ultra-thin flexible 3YSZ substrates, such as thermal conductivity, relative permittivity, dielectric loss, and dielectric breakdown were measured to emphasize its potential applications to electronic packaging. Simulations were employed to demonstrate its comparable thermal resistance in power modules.

## II. Microstructural Analysis

### A. Microstructure of ultra-thin flexible substrate

SEM and EDS were used to analyze the microstructure of the materials, and compared with that of AlN. The sample area is 10mm  $\times$  10mm cut by diamond saw. The SEM images of 3YSZ and AlN substrates are as shown in Fig. 1. It can be seen that the ultra-thin 3YSZ has more uniform and dense microstructure than that of AlN. The shape of 3YSZ grains are round with smaller size, while the shape of AlN grains are columnar with different sizes. The image also indicated that AlN is porous while 3YSZ is dense with very little pores.

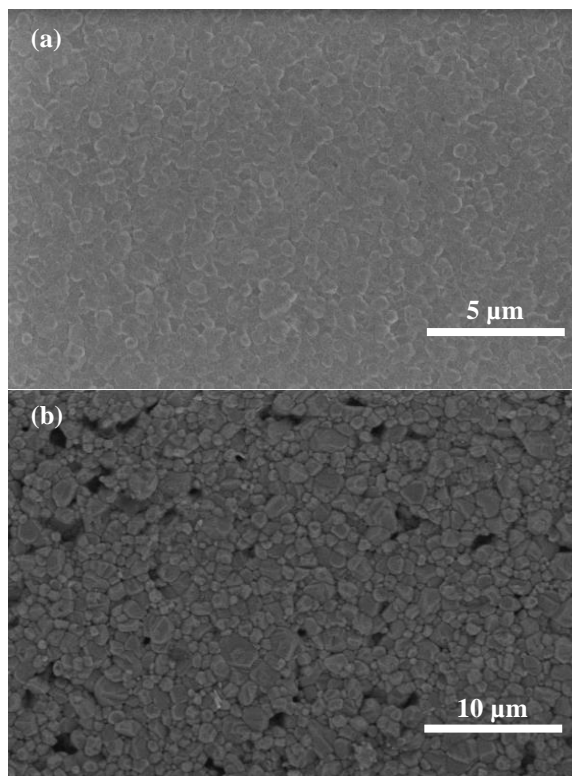


Fig. 1 Microstructure of ceramic substrates: (a) ultra-thin 3YSZ, (b) AlN.

The composition of the ultra-thin flexible 3YSZ substrate was confirmed to contain zirconium, oxygen, yttrium and hafnium by EDS analysis, as shown in Fig. 2.



Fig. 2 Image and X-ray maps of ultra-thin 3YSZ substrate by EDS.

### B. XRD analysis of the ultra-thin flexible substrate

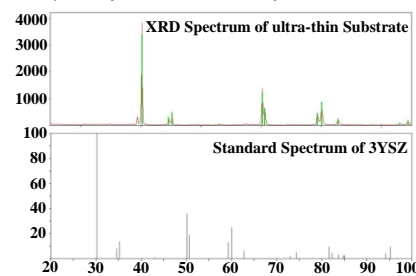


Fig. 3 XRD analysis of ultra-thin flexible 3YSZ substrate.

As shown in Fig. 3, the XRD spectrum of the ultra-thin substrate coincided with the standard spectrum of 3YSZ (O0.984 Y0.065 Zr0.935), according to the PDF card 00-901-5117. The mass fraction of hafnium in the samples was within the natural amount (2% by weight) contained in zirconia [13].

### III. Thermal Conductivity Measurements

#### A. By 3-omega method at different temperatures

The 3-omega method is an AC thermal conductivity technique, with limited errors from back-body radiations even at 1000 K [14] - [15]. A gold heater line was deposited by laser physical vapor deposition (LPVD) on the 40  $\mu\text{m}$  flexible 3YSZ substrate. A Nd-YAG laser beam with wavelength 266 nm, 10 Hz repetition, and variable pulse duration was applied. The deposited pattern on the substrates is shown in Fig. 4. The rectangular pads are for current input and voltage output leads. The heater line width was 100  $\mu\text{m}$ , with effective length 8 mm. Au wires of 0.1 mm was used to connect the heater line on the 3YSZ substrate to the gold pads in a MMR Technology Dewar, with temperature maintained between 80 and 700 K.

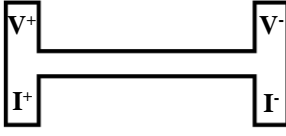


Fig. 4 Schematic of metal pattern deposited by LPVD for gold heater line with electrical terminals.

In the measurement, input ac current, with frequency  $\omega$ , was loaded through the leads, temperature oscillations of the heater line are generated at  $2\omega$ . The temperature change of the heater line is determined by the voltage drop across the heater at  $3\omega$ . The heater works as both a source and thermometer. The resistance of the heater line,  $R$ , and the temperature coefficient of the resistance,  $dR/dT$ , were measured using the four-point probe method. The results showed that the resistance of the heater line at room temperature was 115.18  $\Omega$ , and the temperature coefficient of resistance was 0.20734  $\Omega/\text{K}$ . The temperature increase of the heater at any frequency was calculated by

$$dT = 2V_3 / V_1 (dR/dT) \quad (1)$$

where  $V_3$  is the in-phase value of the third harmonic ( $3\omega$ ) voltage and  $V_1$  is the amplitude of the sinusoidal first harmonic voltage at  $\omega$ .

The thermal conductivity is calculated by

$$K = V_1^3 dR / DT / (4\pi l R^2 \alpha) \quad (2)$$

where  $l$  is the length of heater line,  $\alpha$  is the slope of  $V_3$  against  $\ln(f)$  graph which should be linear [14] - [17].

The values of temperature increase of the heater line per unit power input were simulated using FORTRAN simulations [18]. The numerical values of thermal conductivity and heat capacity of the 3YSZ substrate were determined from the best fit with curves from both experiments and simulations. The experimental and simulated results of increase in temperature of heater line per unit power as function of  $\ln(f)$  at 300 K are shown in Fig. 5. The thermal conductivity of the 3YSZ substrate was found to be 2.7 W/mK.

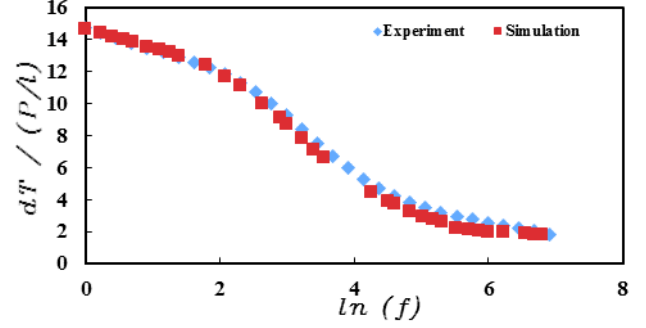


Fig. 5 Curve fitting of increase in temperature of heater line per unit power at room temperature.

Similarly, thermal conductivities of the flexible 3YSZ at temperatures from 235 K to 600 K was measured, It decreased from 3.3 W/mK to 2.2 W/mK, as shown in Fig. 6.

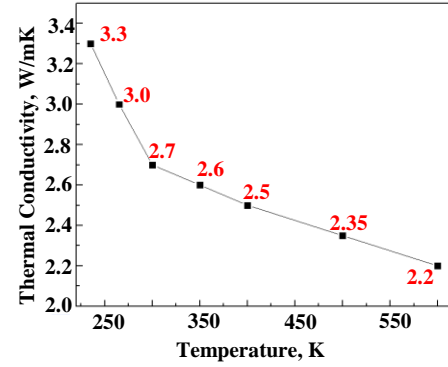


Fig. 6 Thermal conductivity of ultra-thin flexible 3YSZ substrate at different temperatures.

#### B. By transient thermo-reflectance (TTR) method at room temperature

To corroborate the thermal conductivity measurements by three omega method, nanosecond transient thermo-reflectance (TTR) measurement was applied at room temperature. A thin Au tranducerlayer was deposited on the 40  $\mu\text{m}$  3YSZ substrate by LPVD using the same laser source as used for 3-omega measurements. The variation of the temperature on the Au film surface with time is measurements of reflectance from a probe laser shortly after incidence of a pump laser.

Two laser systems were employed in the measurement. A Nd-YAG laser beam (A) with 532 nm wavelength and frequency of 10 Hz, was applied to heat the sample surface. Another continuous laser beam (B) with 650 nm wavelength was applied to measure the transient thermal reflectance (TTR) signal. Both laser beams were focused so that they are incident on the same spot on the surface by passing through a 10 $\times$  objective. A Si photodiode was employed to collect the reflected laser beam B only with pump laser beam. An oscilloscope was used to record the reflected laser beam B collected by laser beam B after amplification. The variation of TTR signal with time was extracted by the oscilloscope signal triggered by output from another Si

detector which also detected the laser beam A before it is incident on the sample surface [19] – [21]. A schematic of TTR equipment setup is as shown in Fig. 7.

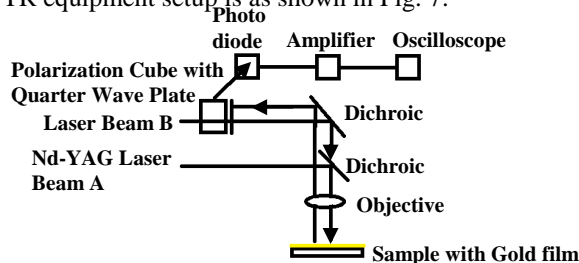


Fig. 7 Schematic of TTR measurement setup.

The normalized variation in TTR signal with time for the Au film, along with curve fitted results from simulations is shown in Fig. 8. The simulation parameters and curve fitting process determined the measured thermal conductivity of the 3YSZ substrate at room temperature, which was 2.85 W/mK. The value agreed with that measured by 3-Omega method well.

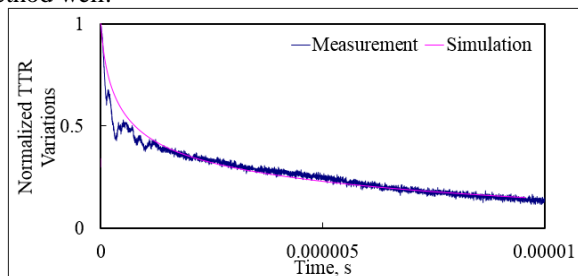


Fig. 8 Curve fitting of Normalized TTR Variation with Time of experimental and simulation results.

### C. Thermal performance of Ultra-thin flexible 3YSZ substrate by simulations

According to these measurements, the thermal conductivity of the ultra-thin flexible 3YSZ substrate was much lower than that of other substrate used for packaging applications, such as  $\text{Al}_2\text{O}_3$  and  $\text{AlN}$ , etc [22] – [24]. Most often, 0.5 mm ~ 0.65 mm thick ceramic plate is used in Cu-clad (e.g. DBC) substrates in power electronic applications. The thicker ceramics are needed for mechanical robustness during circuit assembly, and for stress management during electrical circuits applications.

However, the thickness of 3YSZ substrate was lower, the thermal resistance can be comparable with other materials, especially for power electronics applications. Simulations were performed to compare thermal performance of 3YSZ with  $\text{Al}_2\text{O}_3$  and  $\text{AlN}$  for 2 kV packaging.

The simplified model contains a DBC substrate and a SiC diode attached through Sn-based solder. The parameters and dimension of each part are given in Table. 1.

In the simulation, the power density that the device generated was defined as  $1000\text{W} / \text{cm}^2$ . The bottom temperature of model was set as a constant at  $20^\circ\text{C}$ . The temperature distributions in the models for different ceramic substrates were simulated, and results shown in Fig. 9.

The results showed that the junction temperature of the device on  $40\ \mu\text{m}$  3YSZ was the highest, the results for  $20\ \mu\text{m}$  substrate exhibited an advantage compared to  $\text{Al}_2\text{O}_3$  with about  $10^\circ\text{C}$  lower junction temperature. The  $\text{AlN}$  model showed the lowest junction temperature of all.

Table. 1. Parameters of different parts in Models for Simulations.

Parts	Dimension / $\text{mm}^3$	Heat Capacity / $\text{J/KgK}$	Density / $\text{Kg/m}^3$	Thermal Conductivity / $\text{W/m}^2\text{K}$
SiC Diode	$4 \times 4 \times 0.4$	690	3210	250
Solder	$4 \times 4 \times 0.05$	230	8400	50.9
Cu plate	$12 \times 12 \times 0.127$	385	89200	383.8
3YSZ	$12 \times 12 \times 0.02$ (0.04)	157	6090	2.3
$\text{Al}_2\text{O}_3$	$12 \times 12 \times 0.254$	880	3690	23
$\text{AlN}$	$12 \times 12 \times 0.254$	780	3260	170

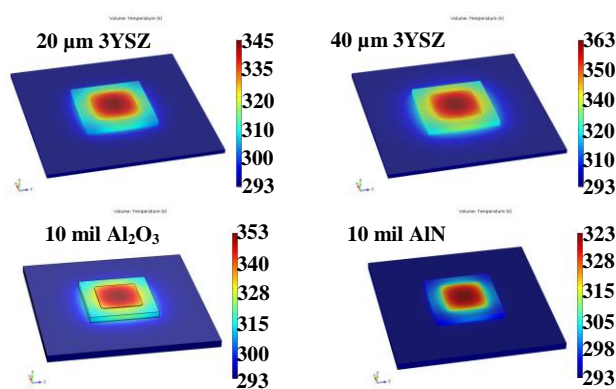


Fig. 9 Thermal Performance of Flexible 3YSZ substrates, compared with  $\text{AlN}$  and  $\text{Al}_2\text{O}_3$ .

## IV. Dielectric Properties

### A. Relative Permittivity and Dielectric Loss

The relative permittivity and dielectric loss was measured as a function of frequency (100 Hz to 1 MHz) and temperature ( $-65^\circ\text{C}$  to  $250^\circ\text{C}$ ). The measurement was setup with a Hewlett Packard 4284 LCR meter and a Delta Design oven model 2300. The oven was equipped with liquid nitrogen so that it can provide both high temperature and low temperature environment in the tests. The bias in the measurements was set as 2Vdc. Platinum electrodes were deposited on both sides of the substrate. The measured dielectric loss and relative permittivity of  $20\ \mu\text{m}$  and  $40\ \mu\text{m}$  3YSZ with temperature and frequency are shown in Fig. 10. The results indicate that the dielectric loss increased slowly with temperature below  $100^\circ\text{C}$  but rapidly for higher temperature. The dielectric loss decreased for higher frequency. Fluctuations on the dielectric loss curve happened after  $150^\circ\text{C}$  at 100 Hz and 1 kHz. Dielectric loss curve of  $40\ \mu\text{m}$  3YSZ substrate coincided with that of the  $20\ \mu\text{m}$  substrate well.

The relative permittivity of 3YSZ also increased slowly with temperature below  $100^\circ\text{C}$  but rapidly for higher

temperature. Also, it decreased with increasing frequency. A drift between results of relative permittivity for 20  $\mu\text{m}$  and 40  $\mu\text{m}$  3YSZ substrates was observed at specific temperature and frequency, as shown in Fig. 10(b).

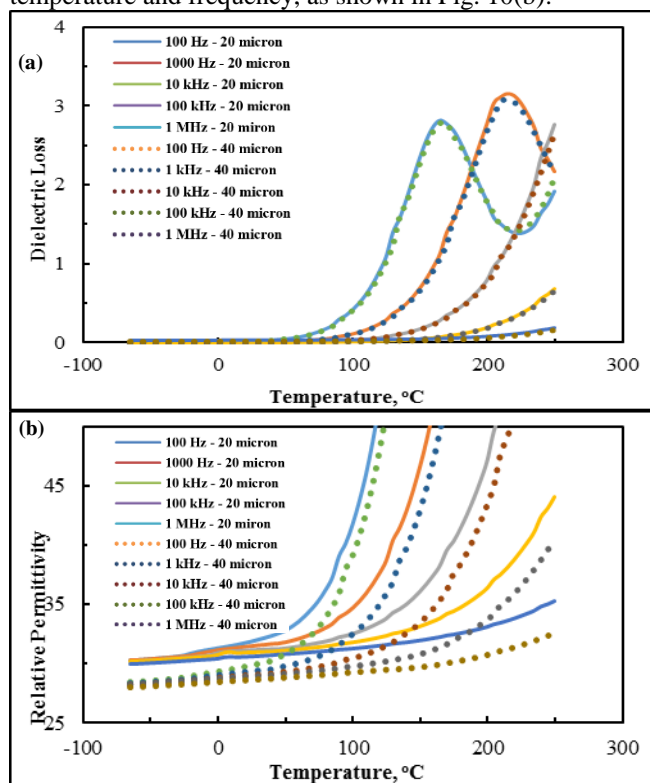


Fig. 10. Dielectric loss (a) and relative permittivity (b) of 20  $\mu\text{m}$  and 40  $\mu\text{m}$  ultra-thin flexible 3YSZ with temperature and frequency.

### B. Dielectric Breakdown

The dielectric breakdown of ultra-thin 3YSZ substrate at different temperatures was measured using a Sawyer-Tower circuit with a Trek high voltage amplifier system. High temperature insulation fluid was employed. During the tests, a DC voltage with ramp rate of 500 V/s was applied until breakdown. The temperature was controlled by a digital hot plate with a thermal couple. The characteristic breakdown strength was determined by the Weibull analysis on 20 sample points in each measurement group. The dielectric strength at measured points for 20  $\mu\text{m}$  and 40  $\mu\text{m}$  is shown in Fig. 11.

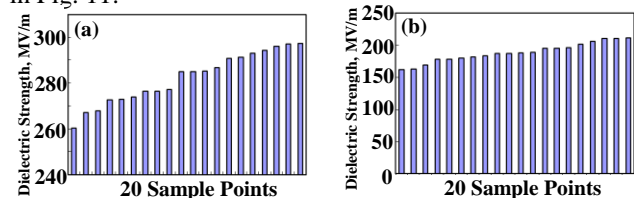


Fig. 11 Measured dielectric strength of different sample points at room temperature: (a) 20  $\mu\text{m}$ , (b) 40  $\mu\text{m}$ .

It is seen from Fig. 11 that a larger variation was found in the dielectric strength of measured points on 20  $\mu\text{m}$  substrate than that on 40  $\mu\text{m}$ . To determine the breakdown

of samples [25], the Weibull plot of each dataset in Fig. 11 was determined and is shown in Fig. 12.

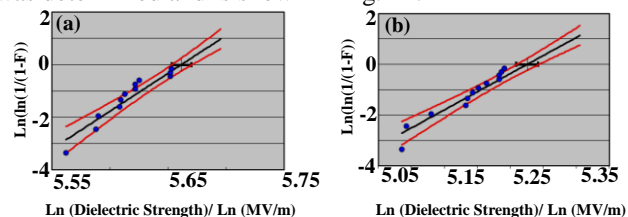


Fig. 12. Weibull Plots of measured data points for dielectric breakdown: (a) 20  $\mu\text{m}$ , (b) 40  $\mu\text{m}$ .

The solid black lines represent the 95% confidence bounds, and the red lines represent ideal breakdown strength distributions. The dielectric breakdown at room temperature was determined, and the results are 288 MV/m for 20  $\mu\text{m}$  substrate and 196 MV/m for 40  $\mu\text{m}$  substrate. Using the same analytical approach, the dielectric strength and breakdown voltage of substrates at 100  $^{\circ}\text{C}$ , 125  $^{\circ}\text{C}$  and 150  $^{\circ}\text{C}$  were determined and summarized in Fig. 13 for the two substrates.

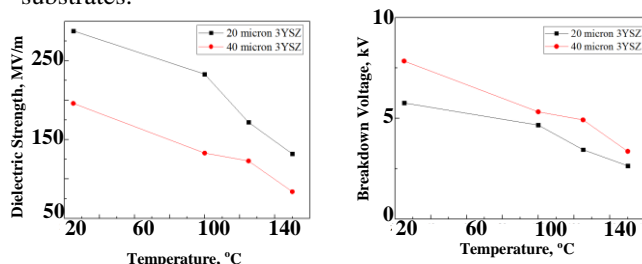


Fig. 13. Dielectric Strength and Breakdown Voltage of ultra-thin 3YSZ. The dielectric strength decreased at higher temperature. A higher electric strength is exhibited at any specific temperature by the YSZ with 20  $\mu\text{m}$  thickness than the YSZ with 40  $\mu\text{m}$  thickness. The 40  $\mu\text{m}$  3YSZ substrate exhibited higher breakdown voltage as its thickness was twice of the thinner 3YSZ substrate. Subsequent testing, not reported here, indicated excessive leakage current for > 100  $^{\circ}\text{C}$  and warrants further investigation.

## V. Discussion

Through the thermal and electrical characterizations, the properties of the ultra-thin flexible 3YSZ substrate were examined to evaluate its potential for electronic packaging applications. The thermal measurements indicated that thermal conductivity was much lower than the conventional AlN and Al<sub>2</sub>O<sub>3</sub> substrates. However, the thermal resistance was still comparable, especially for power electronics applications, with advantages, such as higher power density and better mechanical toughness, to achieve higher power density in 3D packaging structures.

Dielectric loss and relative permittivity measurements indicated that by applying the 3YSZ substrates in the packaging, more losses and more parasitic capacitance would be induced, especially for low frequency and high temperature applications. By applying specific design

layouts in packaging modules, the parasitic capacitance can be utilized as decoupling component.

Dielectric breakdown measurements were achieved by a combination of experimental results and statistical analysis. Though the measured breakdown was acceptable, but the leakage current was questionable.

## VI. Conclusion

This work is part of an explorations into novel materials that can be applied for flexible packaging technologies, especially for flexible power electronics packaging.

The thermal and electrical characterizations of the ultra-thin flexible 3YSZ substrates are reported, including thermal conductivity, dielectric strength, dielectric losses, relative permittivity and composition. Various methods were applied for different measurements and illustrated briefly. And the suitability of the substrates for power electronics devices was discussed based on the measured properties.

## Acknowledgment

This work was covered under contract with Texas Instruments. The author would like to thank the Laboratory for Packaging Research in Electrical Energy Systems (PREES) and MSE department at NCSU, Center for Dielectrics and Piezoelectrics in Penn State for use of their facilities, ENrG Inc. for their E-strate product and technique supports.

## References

- [1] K. S. Kim, Y. K. Lee, Y. H. Kwak, J. H. Park, J. Ha, G. Y. Shin, B. S. Suh, "Novel Substrate Technology for IPM (Intelligent Power Module) Applications: Structural, Thermal and Electrical Characteristics," in *Proc. 14<sup>th</sup> International Conf. Electronic Materials and Packaging, Lantau Island, 2012*, pp. 1-3.
- [2] L. Y. Zhang, Y. F. Zhang, J. Q. Chen, S. L. Bai, "Fluid flow and heat transfer characteristics of liquid cooling microchannels in LTCC multilayered packaging substrate," *International Journal of Heat and Mass Transfer*, vol. 84, Jan. 2015, pp. 339-345.
- [3] Y. Chu, C. Chen, C. Tsou, "A Silicon-Based LED Packaging Substrate With an Island Structure for Phosphor Encapsulation Shaping," *IEEE Transactions on Components, Packaging and Manufacturing Technology*, vol. 5, Feb. 2015, pp. 155-162.
- [4] Y. Wang, L. Overmeyer, "Chip-Level Packaging of Edge-Emitting Laser Diodes Onto Low-Cost Transparent Polymer Substrates Using Optodic Bonding," *IEEE Transactions on Components, Packaging and Manufacturing Technology*, vol. 6, May 2016, pp. 667-674.
- [5] Y. Liu, J. Zhao, C. C. Yuan, G. Q. Zhang, F. Sun, "Chip-on-Flexible Packaging for High-Power Flip-Chip Light-Emitting Diode by AuSn and SAC Soldering," *IEEE Transactions on Components, Packaging and Manufacturing Technology*, vol. 4, Nov. 2016, pp. 1754-1759.
- [6] Z. Chen, H. Y. Hwang, N. Jaafar, D. M. W. Rhee, "Study on power cycling reliability of power module with single metal layer flexible substrate by finite element analysis," *IEEE 17<sup>th</sup> Electronics Packaging and Technology Conf. Singapore, 2015*, pp. 1-7.
- [7] J. G. Bai, G. Q. Lu, X. Liu, "Flip-chip on flex integrated power electronics modules for high density power integration," *IEEE Transactions on Advanced Packaging*, vol. 26, Feb. 2003, pp. 54-59.
- [8] H. Quach, S. S. Ang, F. Barlow, A. Elshabini, K. Olejniczak, A. Malshe, W. D. Brown, "A flip-chip power electronics packaging technology on a flexible polymeric substrate," in *Proc. 3<sup>rd</sup> Electronics Packaging Technology Conference, 2000*, pp. 302-307.
- [9] A. D. Parralejo, A. L. Ortiz, F. R. Rojas, F. Guiberteau, "Effect of N<sub>2</sub> sintering atmosphere on the hardness of sol-gel films of 3 mol% Y<sub>2</sub>O<sub>3</sub>-stabilized ZrO<sub>2</sub>," *Thin Solid Films*, vol. 518, March 2010, pp. 2779-2782.
- [10] I. Garbayo, G. Dezanneau, C. Bogicevic, J. Santiso, I. Gracia, N. Sabate, A. Tarancon, "Pinhole-free YSZ self-supported membranes for micro solid oxide fuel cell applications," *Solid State Ionics*, vol. 216, May 2012, pp. 64-68.
- [11] S. Zhen, W. Sun, G. Tang, D. Rooney, K. Sun, X. Ma, "Fabrication and evaluation of NiO / Y<sub>2</sub>O<sub>3</sub>-stabilized-ZrO<sub>2</sub> hollow fibers for anodes-supported micro-tubular solid oxide fuel cells," *Ceramics International*, vol. 42, May 2016, pp. 8559-8564.
- [12] A. D. Parralejo, A. L. Ortiz, R. Caruso, F. Guiberteau, "Effect of type of solvent alcohol and its molar proportion on the drying critical thickness of ZrO<sub>2</sub>-3 mol% Y<sub>2</sub>O<sub>3</sub> films prepared by the sol-gel method," *Surface and Coating Technology*, vol. 205, Feb. 2011, pp. 3540-3545.
- [13] C. J. Howard, "Structures of the ZrO<sub>2</sub> Polymorphs at Room Temperature by High-Resolution Neutron Powder Diffraction," *Acta Cryst.* 1988, pp. 116-120.
- [14] D. G. Cahill, "Thermal Conductivity measurements from 30 to 750 K: the 3 $\omega$  method," *Review of Scientific Instruments*, vol. 61, Feb. 1990, pp. 802-805.
- [15] D. G. Cahill, Erratum: "Thermal Conductivity measurements from 30 to 750 K: the 3 $\omega$  method," *Review of Scientific Instruments*, vol. 73, Oct. 2002, pp. 3701.
- [16] K. Jagannadham, "Thermal conductivity of AlN-diamond particulate composite films on silicon," *Journal of Vacuum Science & Technology A*, vol. 24, Jul/ Aug 2006, pp. 895-899.
- [17] K. Jagannadham, E. A. Berkman, N. Elmasry, "Thermal conductivity of semi-insulating, p-type, and n-type GaN films on sapphire," *Journal of Vacuum Science & Technology A*, vol. 26, May/June 2008, pp. 375-379.
- [18] J. H. Kim, A. Feldman, D. Novotny, "Application of the Three Omega Thermal Conductivity Measurement Method to a Film on a Substrate of Finite Thickness," *Journal of applied Physics*, vol. 86, May 1999, pp. 3959-3963.
- [19] M. A. Panzer, G. Zhang, D. Mann, X. Hu, E. Pop, H. Dai, K. E. Goodson, "Thermal Properties of Metal-Coated Vertically Aligned Single-Wall Nanotube Arrays," *Journal of Heat Transfer*, vol. 130, May 2008, pp. 052401-1-052401-9.
- [20] H. Zhang, K. Jagannadham, "Interface Thermal Conductance Between Metal Films and Copper," *Metallurgical and Materials Transactions A*, vol. 45A, May 2014, pp. 2480-2486.
- [21] H. Zhang, K. Jagannadham, "Transient thermoreflectance from graphene composites with matrix of indium and copper," *AIP Advance*, vol. 3, 2013, pp. 032111-1-032111-12.
- [22] D. C. Hopkins, T. Baltis, J. M. Pitaressi, D. R. Hazelmyer, "Extreme Thermal Transient Stress Analysis with Pre-Stress in a Metal Matrix Composite Power Package," *High Temperature Electronics Conference (HiTEC)*, Albuquerque, NM, May 2012.
- [23] K. Bhat, Y. B. Guo, Y. Xu, D.R. Hazelmyer, D.C. Hopkins, "Results for an Al/AlN Composite 350°C SiC Solid-State Circuit Beaker Module," *IEEE Applied Power Elect. Conf.*, Orlando, FL, Feb 2012.
- [24] R. Khazaka, L. Mendizabal, D. Henry, R. Hanna. Survey of High-Temperature Reliability of Power Electronics Packaging Components. *IEEE Transactions on Power Electronics*, vol. 30, May 2015, pp.2456-2464.
- [25] E. Y. Wu, R. P. Vollertsen, "On the Weibull Shape Factor of Intrinsic Breakdown on Dielectric Films and Its Accurate Experimental Determination – Part I: Theory, Methodology, Experimental Techniques," *IEEE Transactions on Electron Devices*, vol. 49, Dec. 2002, pp. 2131-2140.